CRYSTALLIZATION OF THE BORON COMPONENT BEARING $MgO-B_2O_3-SiO_2$ SLAG①

Zhang Peixin, Guo Zhenzhong, Lin Hong, Sui Zhitong
Department of Nonferrous Metallurgy,
Northeastern University, Shenyang 110006

ABSTRACT The crystallization and kinetics of the boron component bearing $MgO-B_2O_3-SiO_2$ slag with TiO_2 and ZrO_2 as additive agents were investigated by X-ray diffraction, differential thermal analysis, scanning electron microscopy and infrared ray spectrum. The results showed that additive TiO_2 and ZrO_2 decreased the activation energy of crystallization and improved the phase separation, that make the crystalline phase precipitate easily, the efficiency of extraction of boron (EEB) was promoted. Meanwhile, the structure of slag was modified by addition of TiO_2.

Key words slag containing boron additive agent crystallization

1 INTRODUCTION

A complex ore (ludwigite) containing 30%～35% Fe, 6%～12% B_2O_3, 20%～25% MgO, 12%～15% SiO_2, 1%～2% Al_2O_3 is a very important resource of boron and iron in China. Since the ore was carefully treated by high temperature-chemical process, all of magnesia and 90% boron were concentrated in the molten slags and separated from the liquid pig-iron[1], thus an urgent need is to extract boron from the slags efficiently. It was found that the efficiency of extraction of boron (EEB) was directly related to the precipitating characteristics of the boron component bearing the slag[2], such as in the form of crystalline or amorphous phase. The EEB was high if the boron component existed in the form of crystalline phase, otherwise the EEB was low in the form of amorphous phase. The characteristics of the boron component can be manipulated by additive agents[2]. TiO_2 and ZrO_2 have been mentioned as effective additive agents in many glasses[3-8]. The purpose of the present work is to estimate the influences of additive agents on the crystallization kinetics and crystallization behaviors of the boron component bearing $MgO-B_2O_3-SiO_2$ slag, and to select and optimize the additive agents.

2 EXPERIMENTAL

The chemical composition of 45% MgO, 20% B_2O_3, 35% SiO_2 was selected from chemical reagents with analytical purity. The samples were added by 2% TiO_2 (sample 1), 2% ZrO_2 (sample 2), respectively. Sample 3 was no any additive agent. The samples prepared using the oxide powders as raw materials were put in the graphite crucibles, melted quickly at 1 500 ℃ in the furnace with a $MoSi_2$ heating element and then quenched in cooling water. XRD showed no evidence of crystalline phase existed in the as-quenched samples.

The samples were heated to study their crystallization behaviors. Two methods of heat treatment were employed in this study. The first was that the samples were held at 750 ℃ for 1 h. The second was that the samples were firstly treated at 750 ℃ for 1 h and then were set at 850 ℃ for 30 min.

The precipitated crystalline phase was i-

① Supported by the National Natural Science Foundation of China and the National Doctorate Program Fund of State Education Committee of China; Received Dec. 23, 1994, accepted Mar. 14, 1995

dentified by XRD.

Polished samples were etched with 1% HF and then coated with a thin film of carbon for SEM observations.

The DTA experiments were performed using Shimadia model DT-30B at the heating rates of 5 ℃/min, 10 ℃/min, 20 ℃/min and using α- alumina as the reference.

The IR experiments were carried out with the spectrometer model Nicolet 510P FT-IR.

3 RESULTS AND DISCUSSION

3.1 *Activation Energy of Crystallization*

The crystallization behavior of the slag is similar to that of glass, so it is available to study the crystallization kinetics of the slag by the same method as for glass.

Solid state reaction, such as the crystallization of glass, can be described empirically by the JMA (Johnson-Mehl-Avrami) equation[9, 10]:

$$x = 1 - \exp(-kt^n) \quad (1)$$

where x is the amount of material transformed at the time t, n is a dimensionless quantity called the Avrami exponent, and k is the reaction rate constant, whose temperature dependence is generally expressed by the Arrhenius equation:

$$k = A\exp[-E/RT] \quad (2)$$

where A is the frequency factor, E activation energy, R gas constant, and T Kelvin temperature.

During a DTA experiment the temperature is changed linearly with time at a given rate Φ. The temperature is:

$$T = T_0 + \Phi t \quad (3)$$

where T_0 is the initial temperature and T is the temperature after time t. As the temperature constantly changes with time, k is no longer a constant but varies with time in a more complicated manner:

$$k = A\exp[-E/R(T_0 + \Phi t)] \quad (4)$$

The rate of x reaches its maximum at a temperature T_p. Solving equation (1) for $d^2x/dt^2 = 0$, the following equation is derived as[11-13]:

$$\ln(T_p^2/\Phi) = E/RT_p + \text{const} \quad (5)$$

A plot of $\ln(T_p^2/\Phi)$ vs $1/T_p$ should be a straigt line from which E can be determined from the slope.

One typical DTA curve of the samples at a heating rate of 10 ℃/min is shown in Fig. 1. It can be seen that only one exothermic peak exhibits during the DTA run, the phase identified by XRD showed that the host crystalline phase was $2MgO \cdot B_2O_3$, both $3MgO \cdot B_2O_3$ and $2MgO \cdot SiO_2$ were the minor crystalline phase.

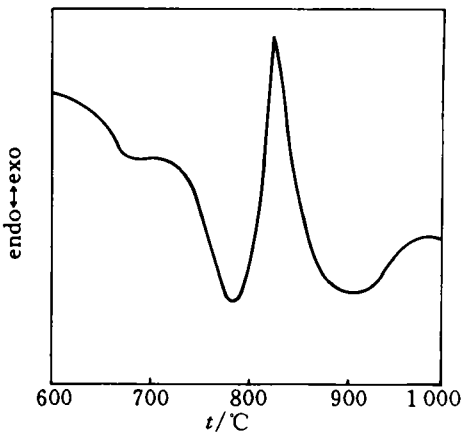

Fig. 1 DTA curve for crystallization of the sample at a heat rate of 10 ℃/min

A plot of $\ln(T_p^2/\Phi)$ versus $1/T_p$ for various samples in Fig. 2 is found to be linear. Values of the activation energy of crystallization E are calculated using Eqn. (5) by least-squares fitting, and $E_1 = 409$ kJ/mol, $E_2 = 421$ kJ/mol, $E_3 = 484$ kJ/mol. It can be indicated that the activation energy of crystallization are remarkably decreased by addition of TiO_2 and ZrO_2. It is suggested that additive agents play an role in weakening glass network and make the boron component precipitate in the form of crystalline phase, thus improving the EEB.

3.2 *Phase Separation and Crystallization*

Fig. 3 shows the micrographs of samples

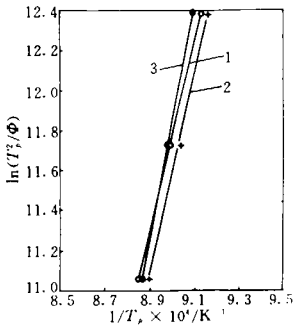

Fig. 2 Plots of $\ln(T_p^2/\Phi)$ vs $1/T_p$ for various samples
1 sample 1; 2 sample 2; 3 sample 3

treated at 750 C for 1 h. The results indicate that the phase separations are observed, but the extent of phase separation for sample 1 and sample 2 is more apparent than sample 3. It is concluded that addition of TiO_2 and ZrO_2 promotes the phase separation. The XRD patterns of samples annealed at 750 C for 1 h and heated at 850 C for 30 min are shown in Fig. 4. The results reveal that the host crystalline phase is $2MgO \cdot B_2O_3$ and the minor crystalline phase is $3MgO \cdot B_2O_3$, in which the amount of crystal of sample 1 are more than that of sample 3. Obviously, addition of TiO_2 improves the precipitation of boron component in the form of $2MgO \cdot B_2O_3$ and $3MgO \cdot B_2O_3$. The precipitated crystals consist of a lot of self-similar dendrites, as shown in Fig. 5.

It is considered[14] that the cations Ti^{4+} and Zr^{4+}, which have small ionic radius and high electric charges as well as great field strength, are prone to polarize the surrounding oxygen anions to form a shield, so that the glass phase separations are accelerated. The phase separations provide the driving force for the nucleation of crystallization and the interface for favourable place to form a crystal nuclei. Even within large supercooling region the phase separations enable the constituents of additive agent to accumulate in one of double phases, and then the crystallites are transformed from the liquid phase as crystal nuclei[15].

During heat treatment the crystallization effect of glass improved by additive agents depends on the quantity and electric charge of cations, since smaller cations with high

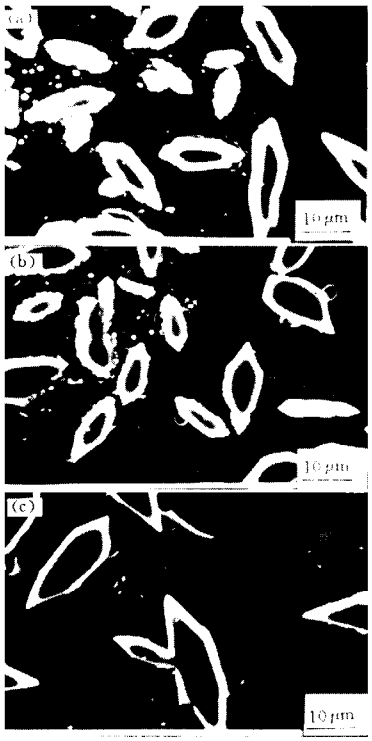

Fig. 3 Microstructures of samples heated at 750 C for 1 h
(a) sample 1; (b) sample 2; (c) sample 3

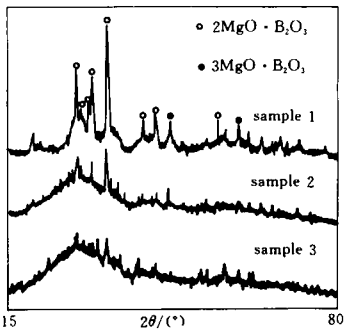

Fig. 4 XRD patterns of samples annealed at 750 C for 1 h and heated at 850 C for 30 min

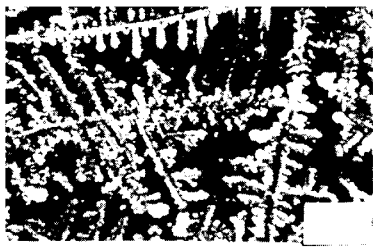

Fig. 5 Microsturcture of sample annealed at 750 C for 1 h and heated at 850 C for 30 min

cationic field strength are more easily surrounded by the oxygen anions, which are arranged in order, than bigger cations with low field strength, so small cations are more prone to be realized transition to order structure of crystal[16]. The field strength of Ti^{4+} ($Z/r^2 = 8.7$) are higher than that of Zr^{4+} ($Z/r^2 = 6.3$)[17], therefore, the activation energy of crystallization are more decreased by TiO_2 than ZrO_2.

3.3 *Structure*

The IR results are shown in Fig. 6. It can be seen that three weak peaks are found in wavenumbers of 490 cm^{-1}, 533 cm^{-1} and 930 cm^{-1} because of addition of TiO_2, they belong to the characteristic vibration of $[B_2O_5]$[18], the curve vibrations of $[BO_3]$ are taken place in the range between 540~590 cm^{-1}, the symmetry expansion and contraction of $[BO_3]$ appear in the range between 900~950 cm^{-1}, the non symmetry expansion and contraction of $[BO_3]$ occur in the range between 1 000~1 260 cm^{-1}[19]. It is suggested that there are a lot of $[B_2O_5]$ and $[BO_3]$ in the slag structures. From the viewpoint of crystal chemistry, the two structures are favourable to make $2MgO \cdot B_2O_3$ and $3MgO \cdot B_2O_3$ precipitate.

4 CONCLUSION

(1) The additives TiO_2 and ZrO_2 decreased the activation energy of crystallization and improved the phase separation, that made

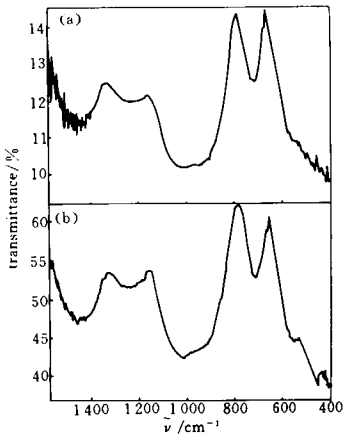

Fig. 6 IR spectra of samples
(a)—sample 1; (b)—sample 3

(To page 78)

60%. It is known from the comparisons in Table 2 that the properties of the deposit produced using the novel technology is obviously better than those of the deposit produced using the conventional technology.

5 CONCLUSIONS

(1) A novel spray deposition technology with the characteristics of multi-layer depostion and the combination of forced external cooling and internal water cooling of the substrate. Compared with the conventional technology, the novel technology exhibits specific advantages, including larger solidification rate, higher dimensional precison and ease to manufacture large preforms.

(2) The optimum deposition conditions of the multi-layer deposition process depend on the spray distance, the motion rates of the substrate and the heating crucible, the overheating degree of the molten alloys, and the mass ratio of gas to molten alloy. Compared with the single spray deposition technology, it is easy for the multi-layer spray deposition to gain optimum deposition conditions.

REFERENCES

1 Singer A. Powder Metall, 1982, 25(4): 195.
2 Singer A *et al.* Met Tech, 1983, 10: 61.
3 Singer A. The Int J of P/M and P/T, 1985, 3: 21.
4 Lawley A *et al.* Spray Forming: Sci, Tech and Appli 1992 P/M world Congress, USA.
5 Chen Zhenhua *et al*. CN95110862X, 1995.
6 Jiang Hong, Chen Zhenhua. Journal of Central-South Institute of Mining and Metallurgy (in Chinese), 1991(Suppl): 95.
7 Zhao Liyin. Master Thesis (in Chinese), Central South University of Technology, 1994.
8 Wu Zhonghai. Master Thesis (in Chinese), Central South University of Technology, 1993.

(Edited by Peng Chaoqun)

(*From page 48*) the crystalline phase easily, thus the EEB was promoted. They are valid additive agents.

(2) The structure of slag was modified by addition of TiO_2. A lot of $[B_2O_5]$ and $[BO_3]$ which were favourable to make the crystal of $2MgO \cdot B_2O_3$ and $3MgO \cdot B_2O_3$ precipitate were produced.

REFERENCES

1 Zhang Peixin *et al.* Liaoning Metallurgy, 1991, (4): 19—22.
2 Zhang Peixin *et al.* Metall Trans B. 1995, 26: 345—356.
3 Doherty P E, Lee D W, Ravis R S. J Am Ceram Soc, 1967, 50: 77—80.
4 Maurer R D. J Appl Phys, 1962, 33: 2132—2139.
5 Hsu J Y, Speyer R S. J Am Ceram Soc, 1989, 72: 2334—2341.
6 Partridge G. Glass Technol, 1982, 23: 133—138.
7 Zdaniewki W. J Am Ceram Soc, 1975, 58: 163—169.
8 Yuan B *et al.* Special Glasses, 1989, 6: 14—17.
9 Jonhson W A, Mahl R F. Trans Amer Inst Min Eng, 1939, 135: 416—420.
10 Avrami M, J Phys Chem, 1939, 7: 1103—1112; 1940, 8: 212—224; 1941, 9: 177—184.
11 Kissinger H E. J Res Nat Bur Stand, 1956, 57: 217—221.
12 Kissinger H E. Anal Chem, 1957, 29: 1702—1706.
13 Bansal N P, Doremas R H. J Thermal Anal, 1984, 29: 115—119.
14 Wang M Q *et al.* Bulletin of Chinese Ceramic Society, (in Chinese) 1983, 2: 17—21.
15 Li J Z. Journal of Chinese Ceramic Society, 1978, 6: 279—289.
16 McMilan P W. Glass Ceramics. (Chinese Edition), Beijing: Building Industry of China Press, 1988: 103.
17 McMilan P W. Glass Ceramics, (Chinese Edition), Beijing: Building Industry of China Press, 1988: 16.
18 Peng W S, Liu G K. Atlases of Infrared Ray of Mineral (in Chinese), Beijing: Science Press, 1982: 179.
19 Yang N R. The Testing Method of Material of Inorganic Non-Metal (in Chinese), Wuhan: Wuhan University of Technology Press, 273.

(Edited by Wu Jiaquan)